Supplement of Atmos. Chem. Phys., 18, 1593–1610, 2018
https://doi.org/10.5194/acp-18-1593-2018-supplement

Atmospheric Chemistry and Physics
Open Access
EGU

Supplement of

Initiation of secondary ice production in clouds

Sylvia C. Sullivan et al.

Correspondence to: Athanasios Nenes (athanasios.nenes@gatech.edu) and Sylvia C. Sullivan (scs2229@columbia.edu)

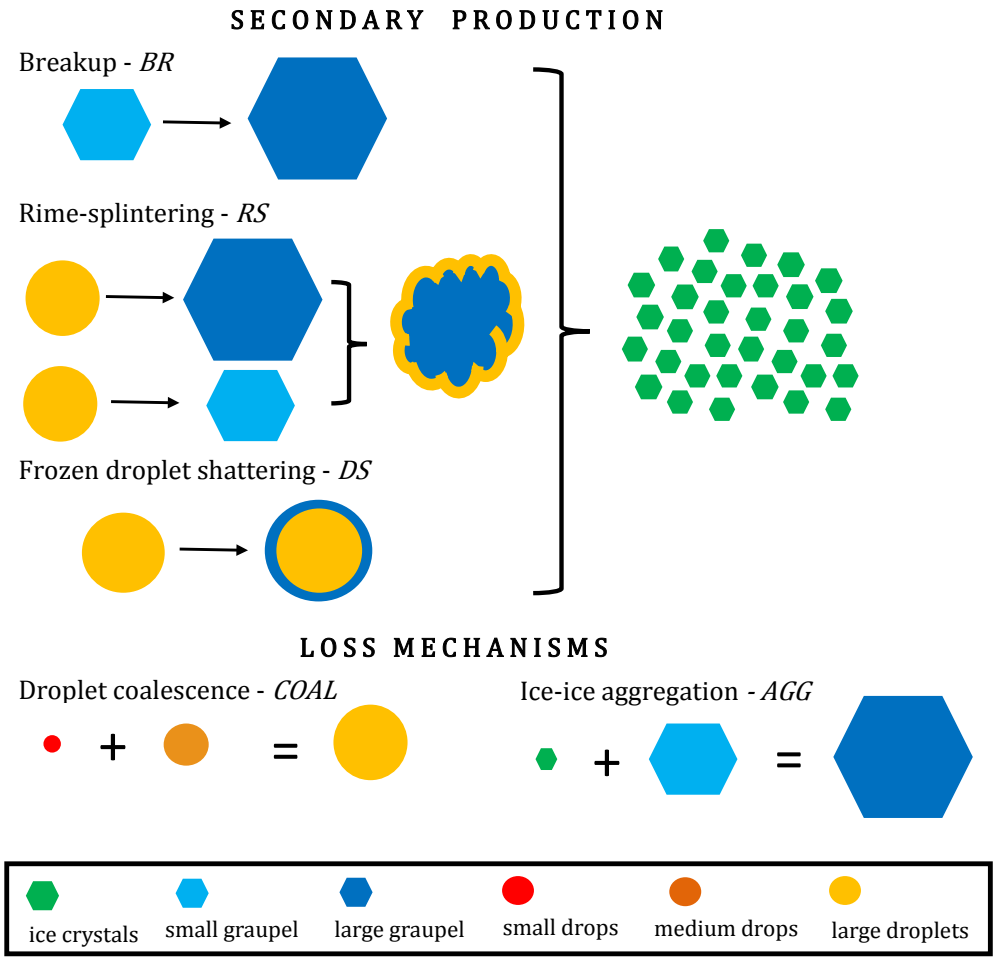

Figure S1. Schematic of the simplified six-bin microphysics model. The secondary production processes included are the collisional breakup of small and large graupel; the rime-splintering of either small or large graupel; or the shattering of large droplets upon freezing. Loss of hydrometeor number occurs through coalescence of small and medium droplets and aggregation of ice crystals and small graupel.

Table S1. Simulations with combinations of processes shown only in Supplemental Information.

Run BRDS	***Run BRRS***	***Run DSRS***
Ice-ice collisional breakup and droplet shattering	Ice-ice collisional breakup and rime splintering	Droplet shattering and rime splintering
$\eta_{RS} = 0\%$	$\eta_{DS} = 0\%$	$\eta_{BR} = 0\%$

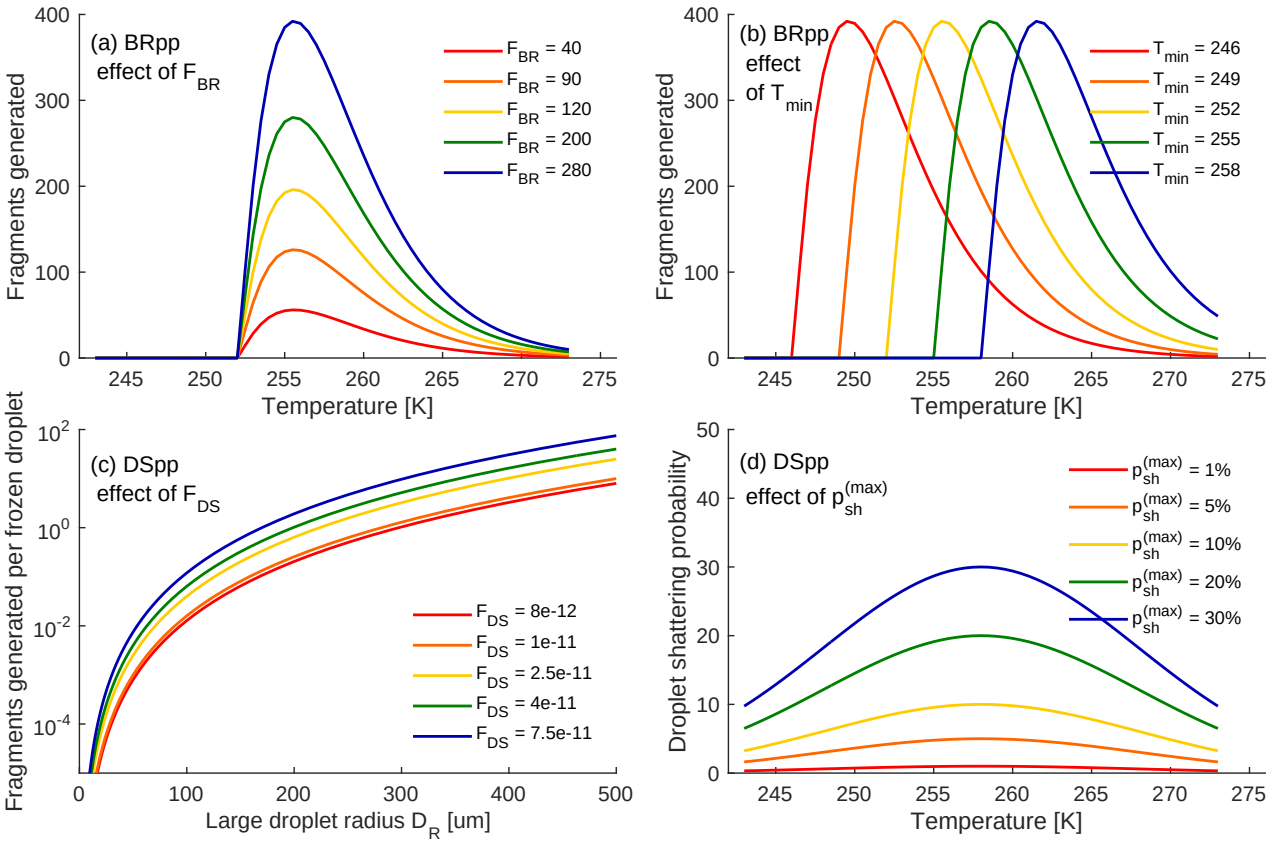

Figure S2. Effect of parameter adjustments with values increasing from red to blue. Panel **(a)** shows the effect of the leading coefficient F_{BR}, and panel **(b)** shows the effect of the minimum temperature of occurrence within the collisional breakup fragment generation function. Panel **(c)** shows the effect of the leading coefficient within the droplet shattering fragment generation function, F_{DS}, while panel **(d)** shows various temperature-dependent shattering probability distributions for the DSpp simulations.

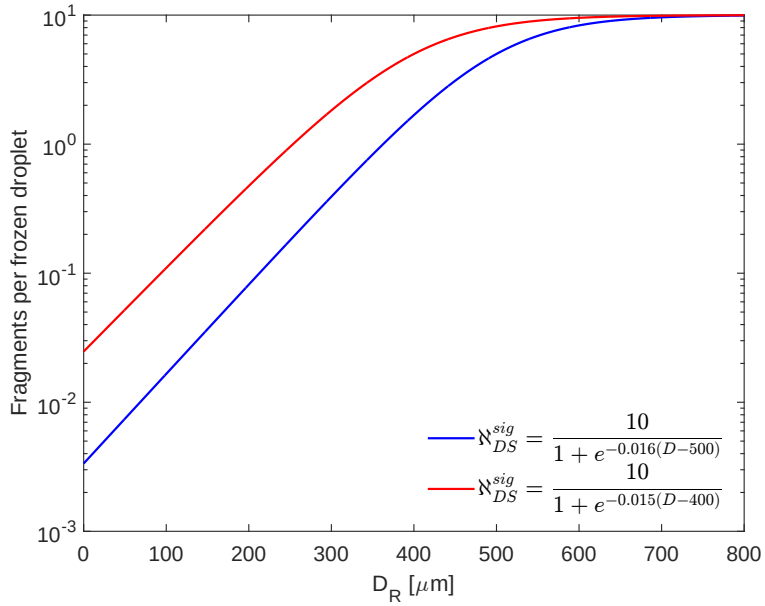

Figure S3. Alternate sigmoidal functions for the fragments generated per frozen droplet as a function of the large droplet diameter.

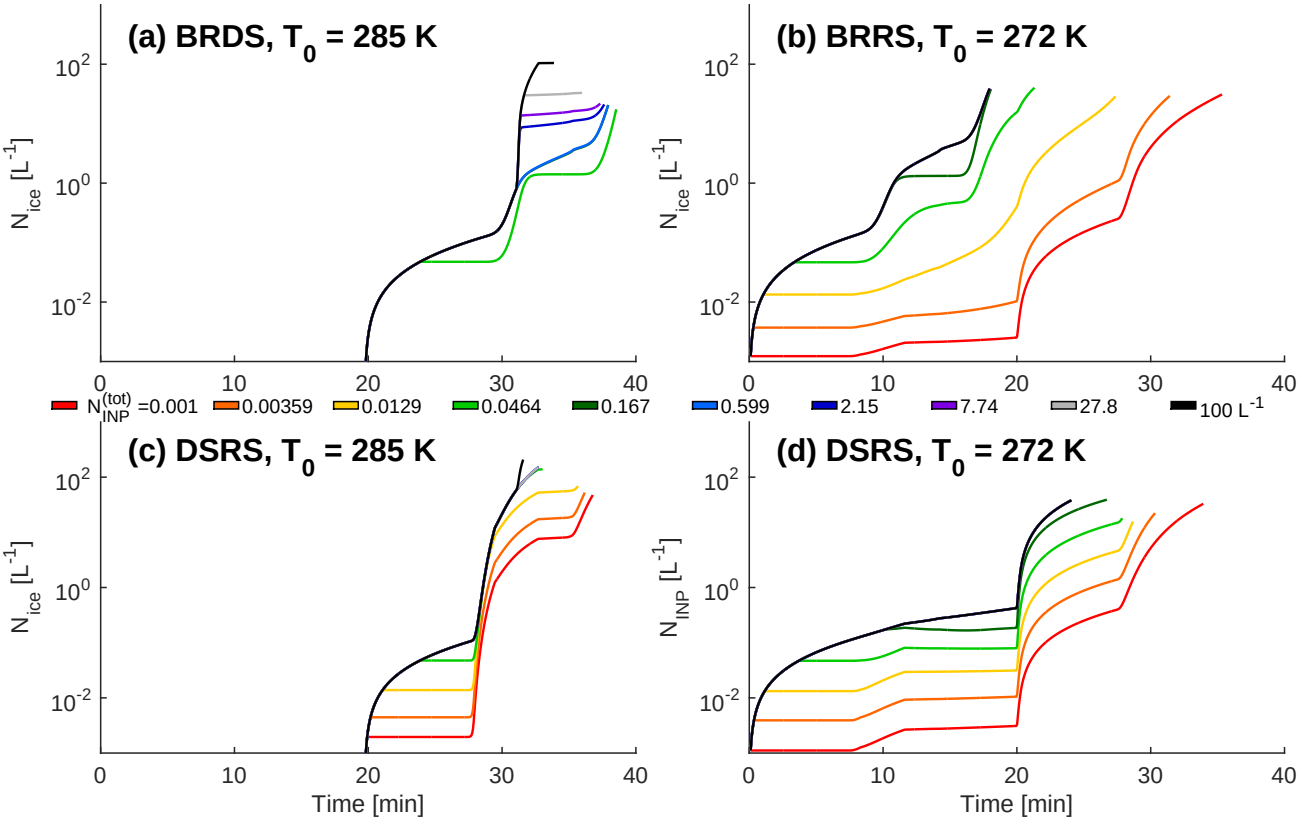

Figure S4. Evolution of the total ice hydrometeor number (summation of ice crystal, small and large graupel numbers) for default simulations with a range of $N_{\mathrm{INP}}^{(tot)}$ from 0.001 up to 100 L^{-1}: **(a)** collisional breakup and droplet shattering from a warmer T_0, **(b)** collisional breakup and rime splintering from a colder T_0, **(c)** droplet shattering and rime splintering from a warmer T_0 and **(d)** from a colder T_0. In panel **(a)**, traces with a smaller $N_{\mathrm{INP}}^{(tot)}$ have been omitted, as they have the same evolution as the DS traces in Figure 1.

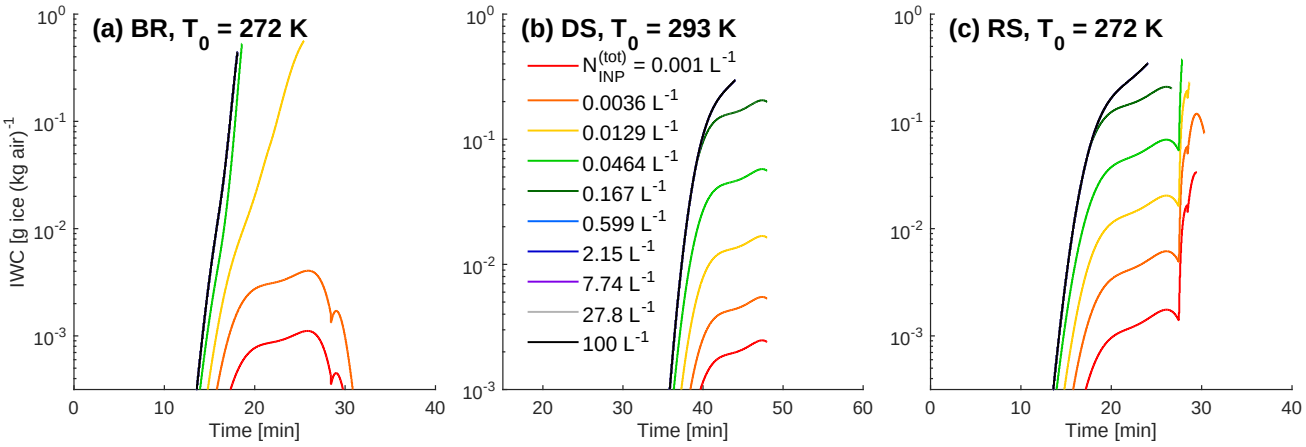

Figure S5. Evolution of the ice mass mixing ratio for default simulations with a range of $N_{\text{INP}}^{(tot)}$ from 0.001 L^{-1} up to 100 L^{-1}: **(a)** ice-ice collisional breakup, **(b)** frozen droplet shattering, and **(c)** rime splintering with initial parcel temperatures T_0 listed.

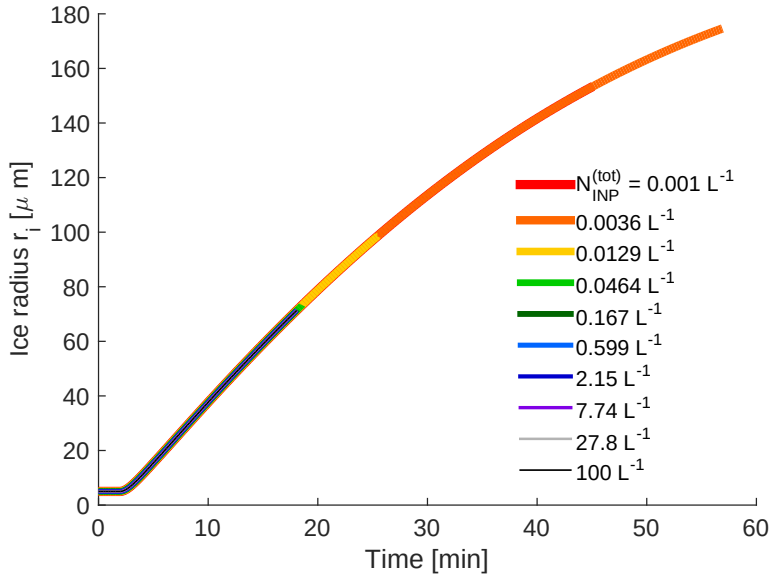

Figure S6. Evolution of the ice crystal radius r_i from the BR simulation with a range of $N_{\text{INP}}^{(tot)}$ from 0.001 L^{-1} up to 100 L^{-1}.